Polymer Journal (2015) 47, 556–563

www.nature.com/pj

ORIGINAL ARTICLE

Crystallization of double crystalline block copolymer/crystalline homopolymer blends: 2. crystallization behavior

Satoru Gondo, Satoshi Osawa, Hironori Marubayashi and Shuichi Nojima

We examined the isothermal crystallization behavior of poly(ε-caprolactone) (PCL) chains (that is, PCL blocks and PCL homopolymers) in binary blends consisting of PCL-*block*-polyethylene (PCL-*b*-PE) copolymers and PCL homopolymers using simultaneous synchrotron small-angle X-ray scattering/wide-angle X-ray diffraction (SAXS/WAXD) and independently using Fourier transform infrared spectroscopy (FTIR). Because the crystallizable temperature of PE blocks was significantly higher than that of PCL chains, the PE block crystallized first upon quenching to form a crystalline lamellar morphology (PE lamellar morphology) and subsequently the PCL chain crystallized within this morphology. We prepared two blends by considering the miscibility of PCL homopolymers in microphase-separated melts; when the PCL homopolymer was localized between PCL blocks in the lamellar microdomain (dry brush), the crystallinity of PCL chains showed a composition-dependent asymptotic increase at the late stage of crystallization, suggesting the individual crystallization of PCL homopolymers and PCL blocks to yield separate PCL lamellar crystals in the PE lamellar morphology. When the PCL homopolymer was uniformly mixed with PCL blocks (wet brush), the time evolution of crystallinity was identical to that of PCL blocks irrespective of composition, indicating that the crystallization of PCL chains was virtually controlled by that of PCL blocks to form a mixed crystal of PCL blocks and PCL homopolymers.
Polymer Journal (2015) **47,** 556–563; doi:10.1038/pj.2015.33; published online 27 May 2015

INTRODUCTION

Many experimental studies have been performed on the crystallization of binary blends consisting of A–B crystalline–amorphous block copolymers and A crystalline homopolymers.[1–14] The crystalline morphology formed in these blends is complicated and hence interesting because it depends significantly on the miscibility of A homopolymers in microphase-separated melts (that is, uniformly mixed or locally segregated). For example, we examined the crystalline morphology formed in binary blends of poly(ε-caprolactone) (PCL)-*block*-polybutadiene copolymers and PCL homopolymers,[4] and found two different morphologies (single lamellar morphology or complex structure of two lamellar morphologies) after crystallization depending on the miscibility of PCL homopolymers.

When B blocks are also crystalline, overall crystallization will be more complicated. That is, when the B block has a higher crystallizable temperature, it crystallizes first upon quenching to form a crystalline lamellar morphology, and eventually A chains (A blocks and A homopolymers) are spatially confined in it before crystallization. This lamellar morphology is a kind of confined space for A chains, and such crystallization will be substantially different from that of polymer chains confined in hard nanodomains.[15–18] This is because the preexisting lamellar morphology consists of hard crystalline lamellae covered with soft amorphous layers and is not sufficiently hard to completely confine the crystallization. Furthermore, this crystallization will be different from those observed in binary blends of crystalline–amorphous diblock copolymers and crystalline homopolymers described above, where the crystallization starts directly from the microphase-separated melt without forming the crystalline lamellar morphology. However, such experimental studies are very limited until now.[19–22] Therefore, it is important to find the crystallization mechanism of A chains on the basis of the miscibility of A chains in the crystalline lamellar morphology.

We have recently examined the crystalline morphology formed in binary blends of PCL-*block*-polyethylene (PCL-*b*-PE) copolymers and PCL homopolymers.[22] The PE block crystallized first upon quenching to form a crystalline lamellar morphology (PE lamellar morphology), where the miscibility of PCL homopolymers in the microphase-separated melt was substantially maintained. Subsequently, the PCL chains (PCL blocks and PCL homopolymers) crystallized within this lamellar morphology. It was found that the resulting morphology depended significantly on the miscibility of PCL homopolymers before crystallization. Namely, when the PCL homopolymer was localized between PCL blocks in the lamellar microdomain structure, separate PCL lamellar crystals (that is, PCL block crystals and PCL

Department of Organic and Polymeric Materials, Graduate School of Science and Engineering, Tokyo Institute of Technology, Tokyo, Japan
Correspondence: Professor S Nojima, Department of Organic and Polymeric Materials, Graduate School of Science and Engineering, Tokyo Institute of Technology, H-125, 2-12-1 Ookayama, Meguro-Ku, Tokyo 152-8552, Japan.
E-mail: snojima@polymer.titech.ac.jp
Received 3 March 2015; revised 17 April 2015; accepted 19 April 2015; published online 27 May 2015

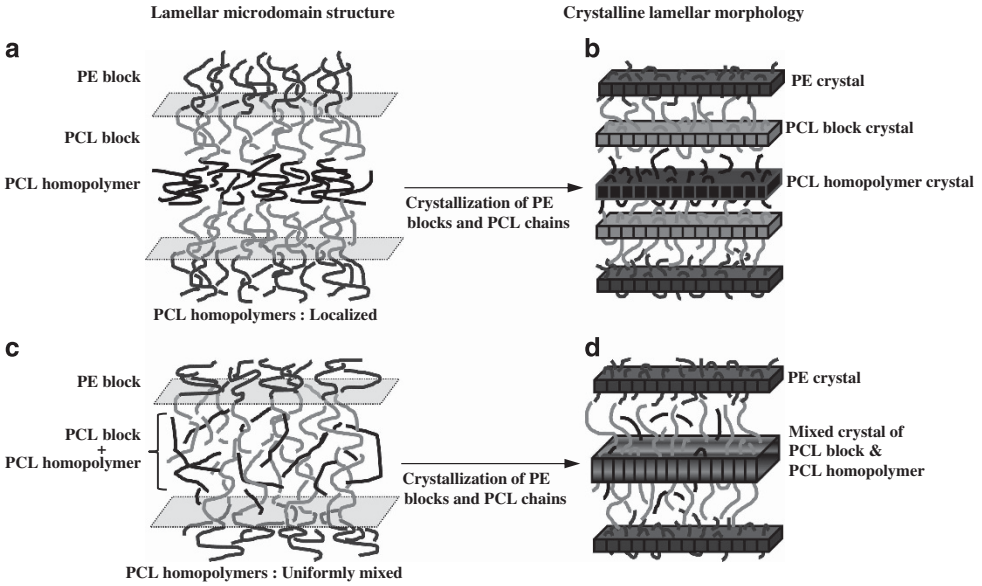

Figure 1 Schematic illustration showing the morphologies formed in binary blends of poly(ε-caprolactone)-*block*-polyethylene (PCL-*b*-PE) copolymers and PCL homopolymers before and after crystallization.[22] The PCL homopolymer is localized between PCL blocks in the lamellar microdomain (**a**) to yield separate PCL crystals after the crystallization of PCL chains (**b**) in the upper route. The PCL homopolymer is uniformly mixed with PCL blocks in the lamellar microdomain (**c**) to form a mixed PCL crystal after the crystallization of PCL chains (**d**).

homopolymer crystals) were formed in the PE lamellar morphology (upper route in Figure 1), whereas when it was uniformly mixed with PCL blocks, a mixed crystal was formed consisting of PCL blocks and PCL homopolymers (lower route in Figure 1).

In this study, we investigate the *crystallization behavior* of PCL chains in the same blends previously used, where the PCL homopolymer exists with different states in lamellar microdomains (that is, uniformly mixed or locally segregated). The crystallization behavior is observed as a function of the volume fraction of PCL homopolymers in PCL chains ϕ_{PCL}. Simultaneous small-angle X-ray scattering (SAXS)/wide-angle X-ray diffraction (WAXD) with synchrotron radiation and independently Fourier transform infrared spectroscopy (FTIR) were employed to pursue the isothermal crystallization process of PCL chains. From these results, we try to find a substantial difference in the crystallization behavior of PCL chains spatially confined in the PE lamellar morphology on the basis of the miscibility of PCL homopolymers in the lamellar microdomain structure. To our knowledge, this is the first time to examine the complicated crystallization of binary blends consisting of crystalline—crystalline diblock copolymers and crystalline homopolymers.

EXPERIMENTAL PROCEDURE

Samples and sample preparation

The crystalline–crystalline block copolymers used in this study are PCL-*b*-PE and the crystalline homopolymer is PCL, both of which are the same samples employed in our previous study.[22] The method used to synthesize these samples has been described elsewhere.[23–25] We synthesized two PCL-*b*-PE copolymers (denoted PCL-PE1 and PCL-PE2) and one PCL homopolymer (PCL), where PCL-PE1: $M_n = 9000$, $M_w/M_n = 1.12$, PCL:PE (vol.%) = 38:62, PCL-PE2: $M_n = 16\,800$, $M_w/M_n = 1.11$, PCL:PE = 51:49, PCL: $M_n = 3000$, $M_w/M_n = 1.05$. It is well known that the molecular weight ratio of PCL homopolymers and PCL blocks r (= M_n(PCL homopolymer)/M_n(PCL block)) controls the miscibility of PCL homopolymers in microphase-separated melts;[26–28] when r is ~1, the PCL homopolymer is locally segregated between PCL blocks, whereas it is uniformly mixed with PCL blocks with $r \ll 1$. Actually, we found in our previous study[22] that the PCL homopolymer was localized between PCL blocks in the lamellar microdomain structure formed in PCL-PE1/PCL blends with $r = 0.83$ (blend 1), and it was homogeneously mixed with PCL blocks in PCL-PE2/PCL blends with $r = 0.33$ (blend 2).

The binary blends with various volume fractions of PCL homopolymers ϕ_{PCL} in PCL chains (PCL blocks and PCL homopolymers) were prepared using a solution-casting method with toluene as a common solvent, where ϕ_{PCL} was calculated using the specific volume of PCL homopolymers[29] and PE homopolymers[30] at 120 °C. The sample thickness was ~2 mm for SAXS/WAXD measurements and 100 μm for FTIR measurements.

Samples were first treated at 120 °C for 15 min to develop microdomain structures in the system, then annealed at 70 °C for >15 min to achieve the complete crystallization of PE blocks and finally quenched to 38 °C to observe the crystallization behavior of PCL chains. It took ~90 s to completely reach to 38 °C during the quenching process. The crystallization temperature (= 38 °C) was chosen by considering that the PE lamellar morphology was virtually maintained after the crystallization of PCL chains below 40 °C,[23,31] and furthermore the crystallization behavior of PCL chains could be conveniently observed using SAXS/WAXD methods.

Simultaneous synchrotron SAXS and WAXD measurements

The crystallization behavior of PCL chains was pursued using simultaneous SAXS and WAXD with synchrotron radiation. The experiment was performed at Photon Factory in High Energy Accelerator Research Organization, Tsukuba, Japan, with a small-angle X-ray equipment for solution installed at BL-10C beam line. Details of the equipment and the instrumentation have already been described elsewhere.[32–34] The two-dimensional SAXS intensity was detected using PILATUS3-2M, which had 1475 × 1679 pixels with 172 × 172 μm^2 in each pixel dimension, and two-dimensional WAXD intensity was simultaneously detected using PILATUS3-200K with 487 × 407 pixels. The accumulation time of one measurement was 10 s during isothermal crystallization for both blends that was continued until the integrated intensity ceased to change. The two-dimensional SAXS and WAXD curves thus measured were azimuthally averaged to obtain one-dimensional SAXS curves as a function of s (= (2/λ) [sin θ], 2θ: scattering angle, λ: X-ray wavelength used (= 0.1488 nm)) and one-dimensional WAXD curves as a function of 2θ, and then corrected for background scattering and absorption by the sample. The PE lamellar morphology existed in the system just before the crystallization of PCL chains, so that it was necessary to subtract the SAXS (or WAXD) curve arising from this lamellar morphology (or PE crystals) to evaluate the substantial change in time-resolved curves due to the crystallization of PCL chains. We simply

subtracted the SAXS (or WAXD) curve at 90 s (corresponding to the curve before the crystallization of PCL chains) from every time-resolved SAXS (or WAXD) curve after 100 s.

Next, the long period L and invariant Q(SAXS) were evaluated as a function of crystallization time t from one-dimensional SAXS curves, and the diffraction intensity I(WAXD) from the (110) plane of PCL crystals from one-dimensional WAXD curves. Finally, we evaluated several parameters characterizing the crystallization behavior of PCL chains in blend 1 and blend 2 as a function of ϕ_{PCL}.

FTIR spectroscopy measurements

FTIR spectra were recorded to examine the crystallization behavior of PCL chains in blend 1 and blend 2 using FTIR 6200 spectrometer (JASCO, Tokyo, Japan) with a spatial resolution of 4 cm^{-1}. The sample was first dissolved in toluene and then thin film (~100 μm in thickness) was prepared by a solution-casting method on a silicone plate. The time evolution of the crystallinity of PCL chains was evaluated from the integrated intensity of absorption band at 934 cm^{-1} resulting from C-O-C symmetric stretching in PCL crystals.[35,36] The normalized crystallinity χ_{PCL}, the integrated intensity at t divided by the final value, was finally evaluated as a function of t during isothermal crystallization at 38 °C, and compared with the results obtained from SAXS or WAXD measurements. It should be noted that the absolute crystallinity of PCL chains, which could not be obtained from SAXS or FTIR measurements, was not important to understand the crystallization behavior, and hence we did not evaluate this value using other methods (for example, differential scanning calorimetry measurements).

RESULTS AND DISCUSSION

Crystallization behavior pursued using SAXS and WAXD

The crystallization process of PCL chains in blend 1 and blend 2 was pursued using simultaneous SAXS/WAXD techniques, and Figure 2 shows the typical time-resolved SAXS (Figure 2a) and WAXD (Figure 2b) curves for blend 1 with $\phi_{PCL} = 0.22$ during isothermal crystallization at 38 °C. The SAXS curve at 120 °C has several scattering peaks arising from the lamellar microdomain structure (not shown in Figure 2a), and turns into another one with diffuse scattering peaks (corresponding to the SAXS curve at $t = 0$ s in Figure 2a) by the crystallization of PE blocks during annealing at 70 °C, indicating a morphological transition from the microdomain structure into some crystalline morphology. This diffuse scattering peak grows remarkably by the subsequent crystallization of PCL chains at 38 °C (shown by an arrow in Figure 2a), where the peak position does not change appreciably. Two distinct scattering peaks (indicated by s^* and $2s^*$) can be observed after the complete crystallization of PCL chains (at $t = 1170$ s), the positions of which exactly correspond to a ratio of 1:2, suggesting a lamellar morphology (that is, an alternating structure consisting of two or more layers) is formed in the system. Of course, the SAXS curves before and after the crystallization of PCL chains ($t = 0$ and 1170 s, respectively) are consistent with those in our previous morphological study using the same samples.[22] It is easily supposed from Figure 2a and our previous studies[23,31] that the PCL chains crystallize within the lamellar morphology formed by the advance crystallization of PE blocks (PE lamellar morphology). The WAXD curves have three appreciable diffraction peaks in Figure 2b. Because the diffraction pattern from PE crystals is extremely similar to that from PCL crystals, these peaks are combined diffractions arising from PE and PCL crystals.

The fundamental parameters characterizing the crystallization process were extracted from SAXS and WAXD curves. Figure 3 shows these parameters as a function of t for blend 1 with $\phi_{PCL} = 0.22$, where data points up to 90 s are omitted by considering the time necessary for quenching. The long period L evaluated from the primary peak position in SAXS curves (Figure 3a) increases slightly at the beginning of crystallization (indicated by a broken line) and thereafter remains nearly constant. It is found from our previous study on the morphology formed in neat PCL-*b*-PE copolymers[31] that PCL blocks crystallize within the existing PE lamellar morphology when the crystallization temperature is <40 °C, although L increases slightly because of the moderate distortion of this morphology. The invariant obtained from SAXS curves Q(SAXS) (Figure 3b) and the (110) diffraction intensity of PCL crystals from WAXD curves I(WAXD) (Figure 3c) both change sigmoidally with increasing t. The increase in Q(SAXS) arises from the large electron density of PCL crystals (= 393 e nm^{-3} [29]) as compared with those of PE crystals (= 340 e nm^{-3} [30]) and amorphous PCL (= 344 e nm^{-3} at 38 °C[29]), and the increase in I(WAXD) from the increase of PCL crystals in the system. Because Q(SAXS) and I(WAXD) are approximately proportional to the crystallinity of PCL chains, the isothermal crystallization behavior of PCL chains is qualitatively similar to that of bulk crystalline homopolymers. Figure 3 clearly indicates that SAXS and WAXD measurements provide the same results for the crystallization behavior of PCL chains, and therefore we mainly analyze the t dependence of Q(SAXS) as a

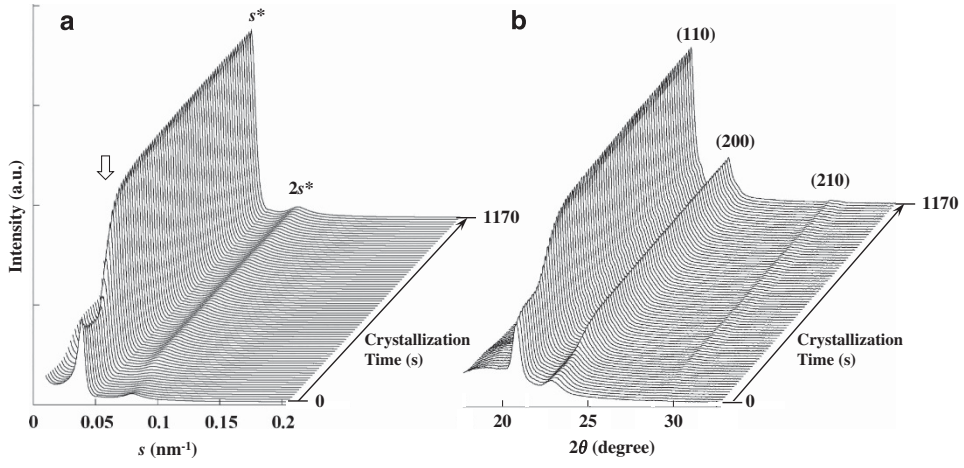

Figure 2 Typical time-resolved (**a**) small-angle X-ray scattering (SAXS) and (**b**) wide-angle X-ray diffraction (WAXD) curves for blend 1 with $\phi_{PCL} = 0.22$ during isothermal crystallization at 38 °C. The s^* in (**a**) represents the wavenumber of primary peak position, and (110), (200) and (210) in (**b**) are the diffraction planes of poly(ε-caprolactone) (PCL) crystals.

function of ϕ_{PCL} to clarify the effects of miscibility of PCL homopolymers (dry brush or wet brush) on the crystallization mechanism of PCL chains.

It should be noted that the crystallization rate of PCL blocks in PCL-PE2 is moderately larger than that of PCL homopolymers because of an advantage of molecular weight (that is, M_n(PCL block) = 9100 and M_n(PCL homopolymer) = 3000), whereas the crystallization rate of PCL blocks in PCL-PE1 (M_n(PCL block) = 3600) is extremely lower than that of PCL homopolymers, in particular at the late stage of crystallization, probably because of the restricted molecular motion of PCL blocks.

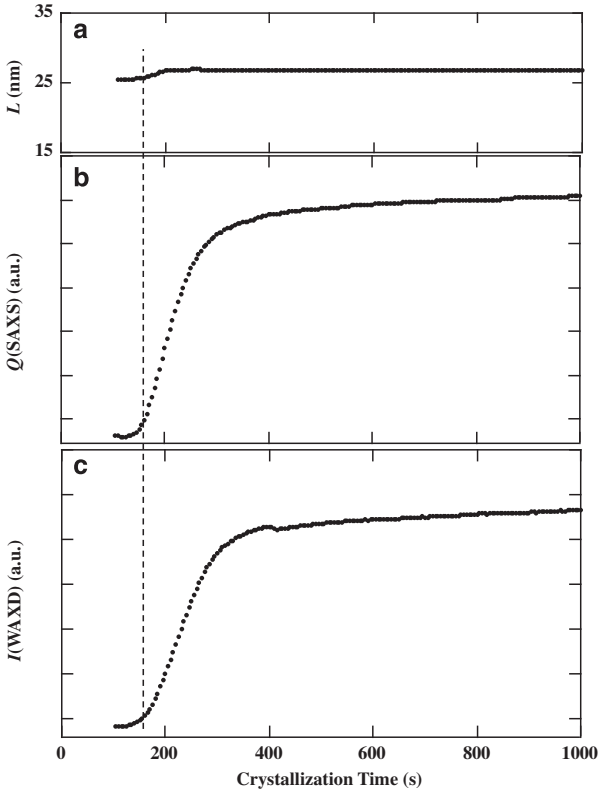

Figure 3 The time evolution of long period L (**a**) and invariant Q(SAXS) (**b**) evaluated from small-angle X-ray scattering (SAXS) curves and (110) diffraction intensity of poly(ε-caprolactone) (PCL) crystals I(WAXD) from wide-angle X-ray diffraction (WAXD) curves for blend 1 with ϕ_{PCL} = 0.22 (**c**) during isothermal crystallization at 38 °C. The broken line represents the crystallization time at which L starts to increase.

Analysis of crystallization behavior

The time evolution of normalized invariant Q'(SAXS) (that is, Q(SAXS) divided by final Q(SAXS)) was analyzed as a function of ϕ_{PCL} to get information on substantial differences in the crystallization mechanism of PCL chains between blend 1 and blend 2. Figure 4 shows Q'(SAXS) plotted against t for blend 1 (Figure 4a) and blend 2 (Figure 4b) with various ϕ_{PCL}. Every crystallization proceeds sigmoidally with a finite induction time that is usually observed for the crystallization of bulk crystalline homopolymers and crystalline blocks confined in lamellar nanodomains.[34,37–39] Furthermore, we find from Figure 4 that the crystallization rate increases steadily with increasing ϕ_{PCL} in blend 1, whereas it is almost the same in blend 2 irrespective of ϕ_{PCL} except that of PCL homopolymers.

The half-time of crystallization $\tau_{1/2}$, the crystallization time at Q'(SAXS) = 0.5, was evaluated to quantitatively compare the crystallization rate, and is plotted in Figure 5 as a function of ϕ_{PCL} for both blends. As easily anticipated from Figures 4, $\tau_{1/2}$ increases extremely with decreasing ϕ_{PCL} at small ϕ_{PCL} for blend 1 to indicate the decelerated crystallization, whereas it remains nearly constant for

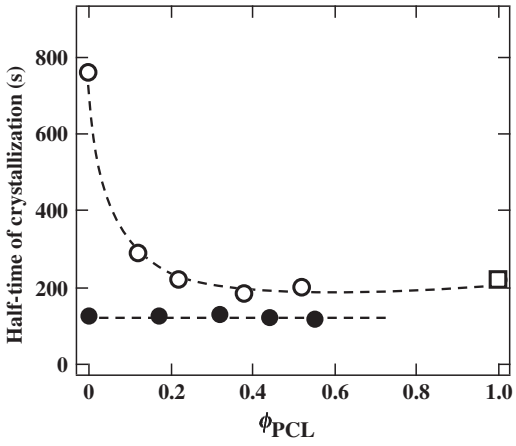

Figure 5 Half-time of crystallization plotted against ϕ_{PCL} for blend 1 (○) and blend 2 (●). The half-time of crystallization at ϕ_{PCL} = 1 (corresponding to poly(ε-caprolactone) (PCL) homopolymers) (□) is common to both blends.

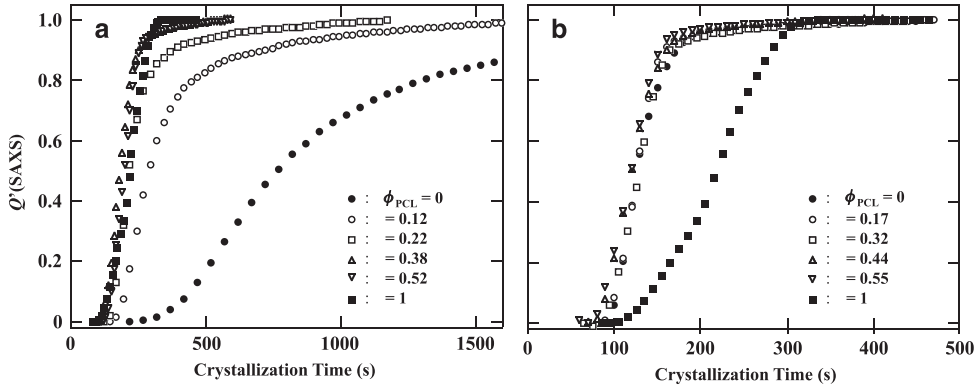

Figure 4 Normalized invariant Q'(SAXS) plotted against crystallization time for blend 1 (dry brush) (**a**) and blend 2 (wet brush) (**b**) both isothermally crystallized at 38 °C. Symbols correspond to different ϕ_{PCL} as shown in each panel. Note that the crystallization time is largely different between blend 1 and blend 2. PCL, poly(ε-caprolactone).

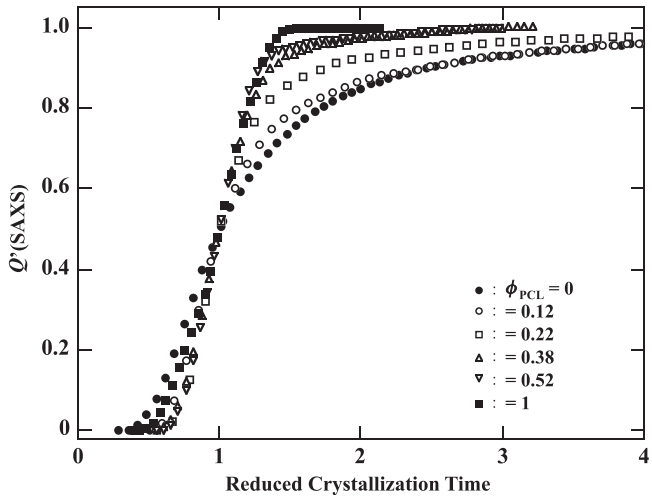

Figure 6 Normalized invariant Q'(SAXS) plotted against reduced crystallization time for blend 1 during isothermal crystallization at 38 °C. Symbols correspond to different ϕ_{PCL} indicated. PCL, poly(ε-caprolactone); SAXS, small-angle X-ray scattering.

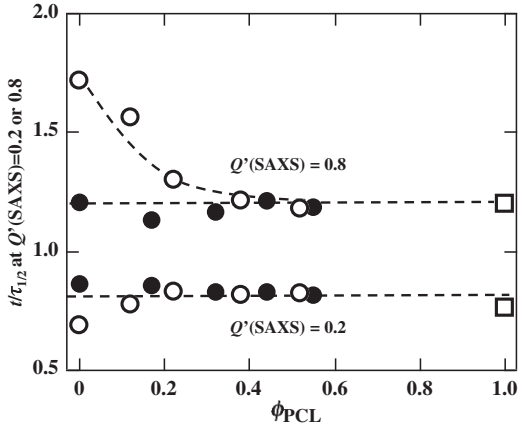

Figure 7 Reduced crystallization time at Q'(SAXS) = 0.2 and 0.8 plotted against ϕ_{PCL} for blend 1 (○) and blend 2 (●). The open squares represent the results of poly(ε-caprolactone) (PCL) homopolymers and are common to both blends. SAXS, small-angle X-ray scattering.

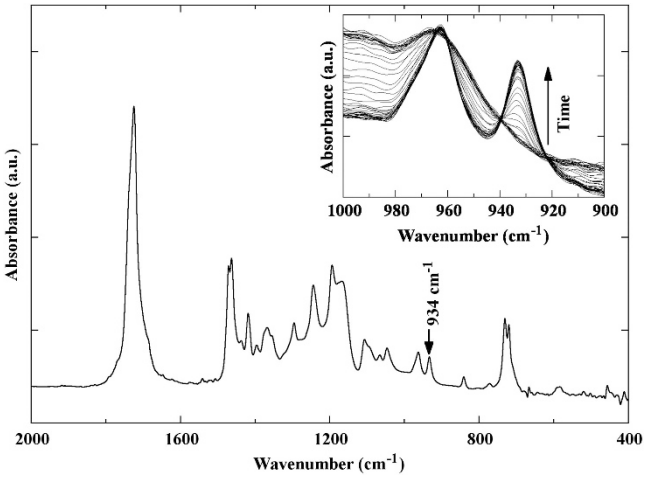

Figure 8 Fourier transform infrared spectroscopy (FTIR) curves of blend 1 with ϕ_{PCL} = 0.22 after complete crystallization at 38 °C. The inset shows the change in FTIR curves during isothermal crystallization at 38 °C for a selected range of wavenumbers. PCL, poly(ε-caprolactone).

blend 2 except that of PCL homopolymers. If PCL homopolymers in blend 2 crystallize separately from PCL blocks, we will have a gradual increase in crystallinity at the late stage of crystallization (and hence a substantial increase in $\tau_{1/2}$) because of the slow crystallization of PCL homopolymers. Therefore, the identical crystallization behavior observed in blend 2 suggests that the crystallization mechanism of PCL chains is completely controlled by the crystallization of long PCL blocks in PCL-PE2 to form a mixed crystal consisting of PCL blocks and PCL homopolymers. This fact is sharply contrasted with the case of blend 1 (Figure 4a), and therefore we further analyze the crystallization behavior of PCL chains in blend 1.

The crystallization time was reduced using $\tau_{1/2}$ in Figure 5 to find the crystallization mechanism of PCL chains in blend 1; if the mechanism is virtually identical, Q'(SAXS) curves make one master curve irrespective of ϕ_{PCL} when plotted against reduced time ($= t/\tau_{1/2}$).[40] Figure 6 shows Q'(SAXS) curves plotted against $t/\tau_{1/2}$ for blend 1 with various ϕ_{PCL}, where they do not make one master curve at the late stage of crystallization ($t/\tau_{1/2} > 1$), indicating that the crystallization mechanism depends intimately on ϕ_{PCL}. We found from our previous study on the crystallization behavior of neat PCL-*b*-polybutadiene copolymers that the crystallization rate of short PCL blocks decelerates significantly at the late stage of crystallization as compared with that of bulk PCL homopolymers, [41] ascribed to the limited diffusion of crystalline blocks.[42,43] Therefore, the ϕ_{PCL}-dependent asymptotic increase in Q'(SAXS) observed at the late stage of crystallization mainly arises from the crystallization of PCL blocks, suggesting the individual crystallization of PCL homopolymers and PCL blocks in blend 1. Namely, the crystallization of PCL homopolymers finishes within a relatively short time ($t/\tau_{1/2} < 2$) but PCL blocks continue to crystallize asymptotically ($t/\tau_{1/2} > 2$). As a result, the $t/\tau_{1/2}$ dependence of Q'(SAXS) reflects two kinds of crystallization (that is, rapid crystallization of PCL homopolymers and slow crystallization of PCL blocks), and the crystallization of PCL blocks is dominant at smaller ϕ_{PCL} ($\leqslant 0.22$), whereas the crystallization of PCL homopolymers at larger ϕ_{PCL} ($\geqslant 0.38$).

The difference in crystallization rates at the early and late stages of crystallization can be clearly found in Figure 7, where the reduced crystallization time at Q'(SAXS) = 0.2 for the early stage of crystallization and Q'(SAXS) = 0.8 for the late stage of crystallization is plotted against ϕ_{PCL} for blend 1 and blend 2. The reduced time at Q'(SAXS) = 0.2 remains nearly constant (~0.75) irrespective of ϕ_{PCL} for both blends, whereas that at Q'(SAXS) = 0.8 for blend 1 is very large at small ϕ_{PCL}. This fact clearly indicates that the characteristics of block copolymer crystallization appear appreciably with decreasing ϕ_{PCL} in blend 1, suggesting the individual crystallization of PCL blocks and PCL homopolymers to form separate PCL lamellar crystals in the PE lamellar morphology.

Crystallization behavior observed using FTIR

We found using simultaneous SAXS/WAXD techniques that the crystallization behavior was substantially different between blend 1 and blend 2 because of the difference in the miscibility of PCL homopolymers in the PE lamellar morphology that originated from the miscibility between PCL homopolymers and PCL blocks in microphase-separated melts. Here, the crystallization behavior of PCL chains in both blends was independently observed using FTIR. Figure 8 shows the typical FTIR curve of blend 1 with ϕ_{PCL} = 0.22 after the complete crystallization of PCL chains at 38 °C, and the inset

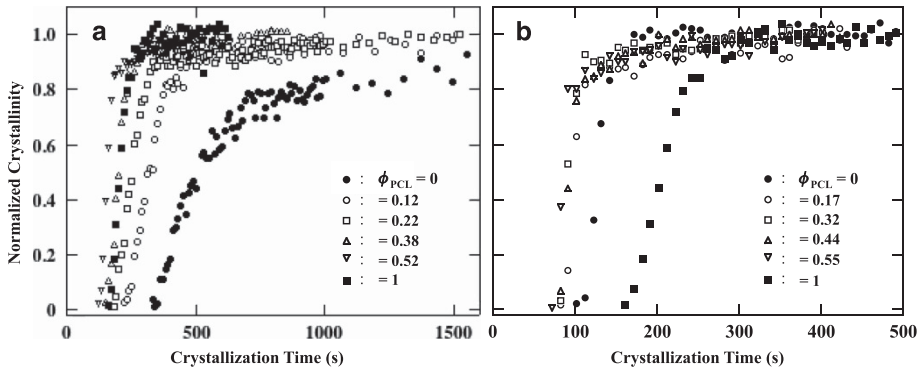

Figure 9 Normalized crystallinities obtained from Fourier transform infrared spectroscopy (FTIR) measurements plotted against crystallization time for blend 1 (**a**) and blend 2 (**b**). Symbols correspond to different ϕ_{PCL}, as shown in each panel. PCL, poly(ε-caprolactone).

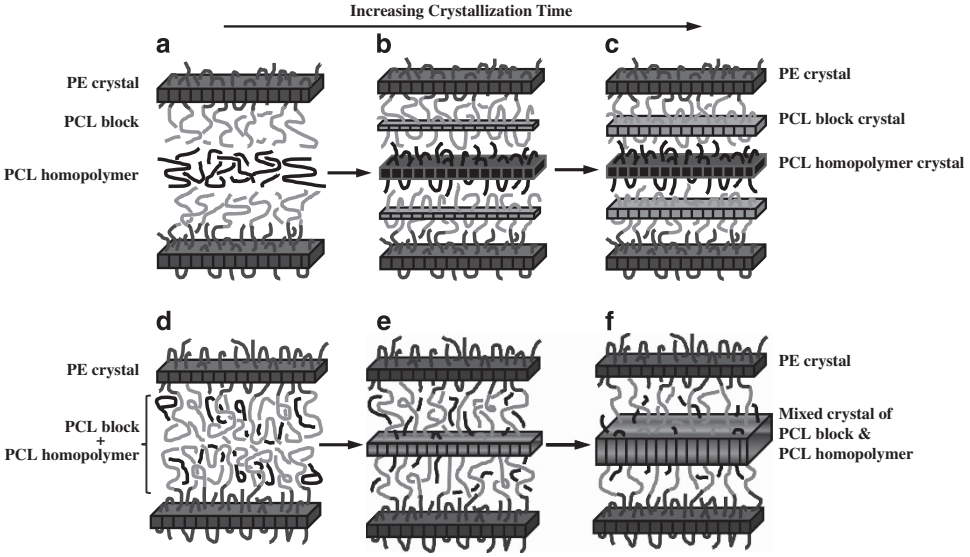

Figure 10 Schematic illustration showing the crystallization process of poly(ε-caprolactone) (PCL) chains in blend 1 (dry brush, upper route) and blend 2 (wet brush, lower route). The lamellar microdomain structure (Figure 1**a** and **c**) is completely replaced with the polyethylene (PE) lamellar morphology (**a**, **d**) by the crystallization of PE blocks, and subsequently PCL chains start to crystallize within this morphology (**b**→**c** in blend 1 and **e**→**f** in blend 2).

represents the change of FTIR curves during isothermal crystallization at 38 °C in a selected range of wavenumbers. We evaluated the normalized crystallinity of PCL chains χ_{PCL} from the steady increase in absorption band at 934 cm^{-1} as a function of t, as precisely described in the Experimental Procedure section.

Figure 9 shows the time evolution of χ_{PCL} during isothermal crystallization at 38 °C for blend 1 (Figure 9a) and blend 2 (Figure 9b) with various ϕ_{PCL} indicated. The data points are generally scattered because the absorption band analyzed is relatively small (Figure 8) and hence much error intervenes for the evaluation of χ_{PCL}. However, the change in χ_{PCL} is extremely similar to that in Q'(SAXS) evaluated using SAXS (and also WAXD) for both blend 1 and blend 2 (Figure 4); the crystallization proceeds sigmoidally irrespective of ϕ_{PCL}. In addition, the crystallization rate of PCL chains in blend 1 increases steadily with increasing ϕ_{PCL} (Figure 9a), whereas it is nearly the same irrespective of ϕ_{PCL} except neat PCL homopolymers in blend 2. Therefore, we easily expect that the analysis of FTIR results leads to the same conclusion derived from simultaneous SAXS/WAXD measurements, and hence we do not analyze the FTIR results anymore. However, it should be noted that the FTIR measurement is important in that it is an alternative method to confirm the crystallization behavior of PCL chains pursued using time-resolved SAXS/WAXD techniques.

Crystallization mechanism of binary blends

In this section, we discuss the crystallization mechanism of PCL chains in blend 1 and blend 2 on the basis of the experimental results obtained using simultaneous SAXS/WAXD and FTIR, and present the schematic change in morphology during the isothermal crystallization of PCL chains. It is important to remember that PCL chains are spatially confined within the PE lamellar morphology throughout crystallization, in which the miscibility of PCL homopolymers is different between blend 1 (dry brush) and blend 2 (wet brush).

Figure 10 shows an illustration showing the change in morphology during the isothermal crystallization of PCL chains in blend 1 (upper route) and blend 2 (lower route). In blend 1, the local segregation of PCL homopolymers from PCL blocks still exists in the PE lamellar morphology (Figure 10a), from which PCL homopolymers and PCL blocks together start to crystallize. However, the PCL block continues to crystallize after finishing the crystallization of PCL homopolymers (Figure 10b→ Figure 10c) because the crystallization rate is significantly different at the late stage of crystallization between PCL blocks

and PCL homopolymers. This fact suggests no cooperative crystallization of PCL blocks and PCL homopolymers to yield separate PCL lamellar crystals (PCL block crystals and PCL homopolymer crystals) in the PE lamellar morphology (Figure 10c).

The crystallization mechanism of PCL chains in blend 2 is completely different from that in blend 1. That is, PCL blocks and PCL homopolymers are uniformly mixed in the PE lamellar morphology before crystallization (Figure 10d), from which a mixed lamellar crystal appears by a cooperative crystallization (Figure 10e) and grows steadily with increasing crystallization time (Figure 10f). This mechanism is easily anticipated from identical crystallization curves irrespective of ϕ_{PCL} (Figure 4b). As a result, the final crystalline morphology formed in blend 2 is substantially different from that in blend 1, as schematically shown in Figures 10c and f. The resulting morphologies derived from the crystallization behavior in this study are consistent with those concluded in our previous study on the final morphology formed in blend 1 and blend 2 examined using static SAXS and thermal analysis.[22]

CONCLUSIONS

We have examined the crystallization behavior of binary blends consisting of PCL-*b*-PE copolymers and PCL homopolymers using simultaneous SAXS/WAXD and independently FTIR as a function of the volume fraction of PCL homopolymers ϕ_{PCL} in PCL chains (that is, PCL blocks and PCL homopolymers). Because the crystallizable temperature of PE blocks was significantly higher than that of PCL chains, the PE block crystallized first upon quenching from microphase-separated melts to form a crystalline lamellar morphology (PE lamellar morphology), followed by the crystallization of PCL chains within this morphology. Two binary blends (denoted blend 1 and blend 2) were prepared by considering the miscibility of PCL homopolymers in microphase-separated melts; the PCL homopolymer was localized between PCL blocks in the lamellar microdomain in blend 1 (dry brush), whereas it was uniformly mixed with PCL blocks in blend 2 (wet brush).

The time evolution of the crystallinity of PCL chains during isothermal crystallization at 38 °C showed a composition-dependent asymptotic increase at the late stage of crystallization in blend 1. The decelerated crystallization of short PCL blocks was responsible for this result, suggesting the individual crystallization of PCL blocks and PCL homopolymers to yield separate PCL lamellar crystals in the PE lamellar morphology. However, the crystallization behavior of blend 2 was virtually identical irrespective of ϕ_{PCL} except that of PCL homopolymers, indicating that morphology formation is controlled by the crystallization of PCL blocks to form a mixed PCL crystal in the PE lamellar morphology. The resulting morphologies formed in blend 1 and blend 2 derived from this study were consistent with those concluded in our previous study using static SAXS and thermal analysis.

ACKNOWLEDGEMENTS

The SAXS measurements were performed under the approval of Photon Factory Advisory Committee (Nos. 2012G041 and 2014G011).

1 Veith, C. A., Cohen, R. E. & Argon, A. S. Morphologies of poly(dimethyl siloxane)-nylon-6 diblock copolymers and blends. *Polymer* **32**, 1545–1554 (1991).
2 Liu, L., Li, H., Jiang, B. & Zhou, E. Compatibility and crystallization of tetrahydrofuran-methyl methacrylate diblock copolymer/polytetrahydofuran blends. *Polymer* **35**, 5511–5517 (1994).
3 Liu, L. Z., Yeh, F. J. & Chu, B. Synchrotron SAXS study of crystallization and microphase separation in compatible mixtures of tetrahydrofuran-methyl methacrylate diblock copolymer and poly(tetrahydrofuran). *Macromolecules* **29**, 5336–5345 (1996).
4 Nojima, S., Kuroda, M. & Sasaki, S. Morphological study on binary blends of poly(ε- caprolactone)-*block*-polybutadiene and poly(ε-caprolactone). *Polym. J.* **29**, 642–648 (1997).
5 Rangarajan, P., Haisch, C. F., Register, R. A., Adamson, D. H. & Fetters, L. J. Influence of semicrystalline homopolymer addition on the morphology of semicrystalline diblock copolymers. *Macromolecules* **30**, 494–502 (1997).
6 Liu, L. Z., Xu, W., Li, H., Su, F. & Zhou, E. Crystallization and intriguing morphologies of compatible mixtures of tetrahydrofuran-methyl methacrylate diblock copolymer with poly(tetrahydrofuran). *Macromolecules* **30**, 1363–1374 (1997).
7 Manaure, A. C. & Müller, A. J. Nucleation and crystallization of blends of poly(propylene) and ethylene/α-olefin copolymers. *Macromol. Chem. Phys.* **201**, 958–972 (2000).
8 Xu, J. T., Fairclough, J. P. A., Mai, S. M., Ryan, A. J. & Chaibundit, C. Isothermal crystallization kinetics and melting behavior of poly(oxyethylene)-*b*-poly(oxybutylene)/poly(oxybutylene) blends. *Macromolecules* **35**, 6937–6945 (2002).
9 Akaba, M. & Nojima, S. Synchrotron SAXS studies on morphology formation in a binary blend of poly(ε-caprolactone) homopolymer and poly(ε-caprolactone)-*block*- polybutadiene copolymer. *Polym. J.* **37**, 464–470 (2005).
10 Akaba, M. & Nojima, S. Temperature dependence of crystallization behavior in a phase-separated blend of poly(ε-caprolactone) homopolymer and poly(ε-caprolactone)-*block*-polybutadiene copolymer. *Polym. J.* **38**, 559–566 (2006).
11 Takeshita, H., Gao, Y. J., Natsui, T., Rodriguez, E., Miya, M., Takenaka, K. & Shiomi, T. Formation of phase structure and crystallization behavior in blends containing polystyrene-polyethylene block copolymers. *Polymer* **48**, 7660–7671 (2007).
12 Takeshita, H., Gao, Y. J., Takata, Y., Takenaka, K., Shiomi, T. & Wu, C. Formation of phase structure and crystallization behavior from disordered melt for ethylene-isoprene block copolymers and their blends. *Polymer* **51**, 799–806 (2010).
13 Yu, P. Q., Yan, L. T., Chen, N. & Xie, X. M. Confined crystallization behaviors and phase morphologies of PVCH-PE-PVCH/PE homopolymer blends. *Polymer* **53**, 4727–4736 (2012).
14 Cambridge, G., Gonzalez-Alrarez, M. J., Guerin, G., Manners, I. & Winnink, M. A. Solution self-assembly of blends of crystalline-coil polyferrocenylsilane-*block*- polyisoprene with crystallizable polyferrocenylsilane homopolymer. *Macromolecules* **48**, 707–716 (2015).
15 Lin, M. C., Nandan, B. & Chen, H. L. Mediating polymer crystal orientation using nano-templates from block copolymer microdomains and anodic oxide nano-channels. *Soft Matter* **8**, 7306–7322 (2012).
16 He, W. N. & Xu, J. T. Crystallization assisted self-assembly of semicrystalline block copolymers. *Prog. Polym. Sci.* **37**, 1350–1400 (2012).
17 Michell, R. M., Blaszczyk-Lezak, I., Mijangos, C. & Müller, A. J. Confinement effects on polymer crystallization: from droplets to alumina nanoporos. *Polymer* **54**, 4059–4077 (2013).
18 Jiang, Q. & Ward, M. D. Crystallization under nanoscale confinement. *Chem. Soc. Rev.* **43**, 2066–2079 (2014).
19 Harrats, C., Fayt, R. & Jerome, R. Synthesis and compatibilization ability of hydrogenated polybutadiene-*b*-polyamide 6 diblock copolymer in low density polyethylene and polyamide 6 blends. *Polymer* **43**, 5347–5354 (2002).
20 Castillo, R. V. & Müller, A. J. Crystallization and morphology of biodegradable or biostable single and double crystalline block copolymers. *Prog. Polym. Sci.* **34**, 516–560 (2009).
21 Salim, N. V., Hanley, T. & Guo, Q. Microphase separation through competitive hydrogen bonding in double crystalline diblock copolymer/homopolymer blends. *Macromolecules* **43**, 7695–7704 (2010).
22 Gondo, S., Osawa, S., Sakurai, T. & Nojima, S. Crystallization of double crystalline block copolymer/crystalline homopolymer blends: 1. Crystalline morphology. *Polymer* **54**, 6768–6775 (2013).
23 Nojima, S., Akutsu, Y., Washino, A. & Tanimoto, S. Morphology of melt-quenched poly(ε-caprolactone)-*block*-polyethylene copolymers. *Polymer* **45**, 7317–7324 (2004).
24 Nojima, S., Kiji, T. & Ohguma, Y. Characteristic melting behavior of double crystalline poly(ε-caprolactone)-*block*-polyethylene copolymers. *Macromolecules* **40**, 7566–7572 (2007).
25 Sakurai, T., Nagakura, H., Gondo, S. & Nojima, S. Crystallization of poly(ε-caprolactone) blocks confined in crystallized lamellar morphology of poly(ε-caprolactone)-*block*-polyethylene copolymers: effects of polyethylene crystallinity and confinement size. *Polym. J.* **45**, 436–443 (2013).
26 Hashimoto, T., Tanaka, H. & Hasegawa, H. Ordered structure in mixtures of a block copolymer and homopolymers. 2. Effects of molecular weights of homopolymers. *Macromolecules* **23**, 4378–4386 (1990).
27 Tanaka, H., Hasegawa, H. & Hashimoto, T. Ordered structure in mixtures of a block copolymer and homopolymers. 1. Solubilization of low molecular weight homopolymers. *Macromolecules* **24**, 240–251 (1991).
28 Hamley, I. W. *The Physics of Block Copolymers* (Oxford University Press, Oxford, 1998).
29 Crescenzi, V., Manzini, G., Calzolari, G. & Borri, C. Thermodynamics of fusion of poly-β-propiolactone and poly-ε-caprolactone. Comparative analysis of the melting of aliphatic polylactone and polyester chains. *Eur. Polym. J.* **8**, 449–463 (1972).
30 Brandrup, J. & Immergut, E. H. *Polymer Handbook 3rd edn* (Wiley, New York, 1989).
31 Nojima, S., Akutsu, Y., Akaba, M. & Tanimoto, S. Crystallization behavior of poly(ε-caprolactone) blocks starting from polyethylene lamellar morphology in poly(ε-caprolactone)-*block*-polyethylene copolymers. *Polymer* **46**, 4060–4067 (2005).

32 Nojima, S., Tsutsui, H., Urushihara, M., Kosaka, W., Kato, N. & Ashida, T. A dynamic study of crystallization of poly(ε-caprolactone) and poly(ε-caprolactone)/poly(vinyl chloride) blend. *Polym. J.* **18**, 451–461 (1986).
33 Nojima, S., Fukagawa, Y. & Ikeda, H. Interactive crystallization of a strongly segregated double crystalline block copolymer with close crystallizable temperatures. *Macromolecules* **42**, 9515–9522 (2009).
34 Nakagawa, S., Tanaka, T., Ishizone, T., Nojima, S., Kamimura, K., Yamaguchi, K. & Nakahama, S. Crystallization behavior of poly(ε-caprolactone) chains confined in lamellar nanodomains. *Polymer* **55**, 4394–4400 (2014).
35 Verma, D., Katti, K. & Katti, D. Experimental investigation of interfaces in hydroxy apatite/polyacrylic acid/poly caprolactone composites using photoacoustic FTIR spectroscopy. *J. Biomed. Mater. Res.* **77A**, 59–66 (2006).
36 Hagemann, H., Snyder, R. G., Peacock, A. J. & Mandelkern, L. Quantitative infrared methods for the measurement of crystallinity and its temperature dependence: polyethylene. *Macromolecules* **22**, 3600–3606 (1989).
37 Ho, R. M., Lin, F. H., Tsai, C. C., Lin, C. C., Ko, B. T., Hsiao, B. S. & Sics, I. Crystallization –induced undulated morphology in polystyrene-*b*-poly(L-lactide) block copolymer. *Macromolecules* **37**, 5985–5994 (2004).
38 Sun, Y. S., Chung, T. M., Li, Y. J., Ho, R. M., Ko, B. T., Jeng, U. S. & Lotz, B. Crystalline polymers in nanoscale 1D spatial confinement. *Macromolecules* **39**, 5782–5788 (2006).
39 Sun, Y. S., Chung, T. M., Lin, Y. J., Ho, R. M., Ko, B. T. & Jeng, U. S. Crystal orientation within lamellae-forming block copolymers of semicrystalline poly(4-vinylpyridine)-*b*-poly(ε-caprolactone). *Macromolecules* **40**, 6778–6781 (2007).
40 Nojima, S., Kato, K., Ono, M. & Ashida, T. Time-resolved SAXS study of morphological change in a binary blend of poly(ε-caprolactone) and polystyrene oligomer. *Macromolecules* **25**, 1922–1928 (1992).
41 Nojima, S., Nakano, H., Takahashi, T. & Ashida, T. Crystallization of block copolymers: 3. Crystallization behavior of an ε-caprolactone-butadiene diblock copolymer. *Polymer* **35**, 3479–3486 (1994).
42 Kundu, C. & Dasmahapatra, A. K. Crystallization of double crystalline symmetric diblock copolymers. *Polymer* **55**, 958–969 (2014).
43 Ueda, M., Sakurai, K., Okamoto, S., Lohse, D., MacKnight, W. J., Shinkai, S., Sakurai, S. & Nomura, S. Spherulite formation from microphase-separated lamellae in semi-crystalline diblock copolymer comprising polyethylene and atactic polypropylene blocks. *Polymer* **44**, 6995–7005 (2003).